The *pineapple eye* Gene Is Required for Survival of Drosophila Imaginal Disc Cells

Wei Shi, Argyrios Stampas, Cynthia Zapata and Nicholas E. Baker[1]

Department of Molecular Genetics, Albert Einstein College of Medicine, Bronx, New York 10461

Manuscript received April 10, 2003
Accepted for publication August 12, 2003

ABSTRACT

Each ommatidium of the Drosophila eye is constructed by precisely 19 specified precursor cells, generated in part during a second mitotic wave of cell divisions that overlaps early stages of ommatidial cell specification. Homozygotes for the *pineapple eye* mutation lack sufficient precursor cells due to apoptosis during the period of fate specification. In addition development is delayed by apoptosis during earlier imaginal disc growth. Null alleles are recessive lethal and allelic to *l(2)31Ek*; heteroallelic combinations can show developmental delay, abnormal eye development, and reduced fertility. Mosaic clones autonomously show extensive cell death. The *pineapple eye* gene was identified and predicted to encode a novel 582-amino-acid protein. The protein contains a novel, cysteine-rich domain of 270 amino acids also found in predicted proteins of unknown function from other animals.

IN Drosophila as in other organisms, development of the adult from the egg is associated with both specification of diverse cell types and increased cell number and body size. Differentiation and patterning of many body regions have been intensively studied. Mechanisms of growth and proliferation are a more recent focus (Oldham *et al.* 2000; Edgar *et al.* 2001; Johnston and Gallant 2002). Many adult fly structures derive from so-called imaginal discs, embryonic cells that are set aside to proliferate and grow during larval life without differentiating until metamorphosis, when they replace the larva with adult structures within the pupa. Larval life occurs largely independently of imaginal discs, so that defects in imaginal disc growth or patterning can be detected from their later effects on adult structures. The compound eye is an adult structure for which cell number is particularly crucial, because the very regular eye structure depends on precise numbers and arrangements of multiple specialized retinal cell types. For this reason defects in compound eye morphology can be an indication of altered cell proliferation or survival.

The compound eye of Drosophila is composed of hundreds of nearly identical ommatidia or unit eyes (Wolff and Ready 1993). Both the number and the type of cells in ommatidia are invariant. Each ommatidium is constructed by 19 progenitor cells; 18 are specified postmitotically and 1 continues dividing to form a bristle organ. Ommatidial progenitor cells are specified by cell-cell interactions in the eye imaginal disc, the epithelium that gives rise to the eye and head. Cell fate specification begins at the posterior margin of the eye imaginal disc, progressing anteriorly as a "morphogenetic furrow" moves across the eye disc epithelium. Anterior to the morphogenetic furrow, cells in the eye imaginal disc proliferate. The cell cycle arrests in the morphogenetic furrow, and the first 5 cells of each ommatidium are specified. The remaining cells reenter the cell cycle in the "second mitotic wave" posterior to the morphogenetic furrow and later give rise to the other 14 precursor cell types. The second mitotic wave (SMW) makes an important contribution to the number of cells per ommatidium. The number of ommatidia is already fixed by prior specification of the 5-cell preclusters, so that if the SMW is prevented by targeted expression of the cell cycle inhibitor $p21^{WAF1/CIP1}$ then defective ommatidia are generated from the depauperate pool of progenitor cells. By contrast, changes in growth and proliferation anterior to the morphogenetic furrow are likely to lead to changes in the number of ommatidial preclusters and so to larger or smaller eyes containing more or fewer ommatidia, each constructed from the normal complement of precursor cells (de Nooij and Hariharan 1995; Baker 2001; Neufeld and Hariharan 2002).

Ommatidia that assemble in the absence of sufficient precursor cells lack some cells and are unable to stack into the crystalline lattice typical of the normal eye. Such eyes have a roughened, irregular eye surface (de Nooij and Hariharan 1995). The phenotype is associated with variable ommatidial defects. Often later ommatidial cell fates cannot be specified, such as pigment cells that normally function to separate ommatidia into

Sequence data from this article have been deposited with the EMBL/GenBank Data Libraries under accession nos. AF247499–AF247501.

[1]*Corresponding author:* Department of Molecular Genetics, Albert Einstein College of Medicine, 1300 Morris Park Ave., Bronx, NY 10461. E-mail: baker@aecom.yu.edu

individual facets. In this case multiple ommatidia, each perhaps deficient in particular cell types, share oversized facets (de Nooij and Hariharan 1995).

This phenotype of GMRp21$^{WAF1/CIP1}$ resembles that of mutations in an endogenous Drosophila gene, *pineapple eye*. Ommatidia from *pineapple eye* (*pie*) mutants initiate development normally, but become increasingly defective, and cell types that are specified later in the cascade such as cone cells, pigment cells, and some photoreceptor cells are often missing (Baker *et al.* 1992). The *pie* adults have roughened and irregular eyes with large facets like those described for GMRp21$^{WAF1/CIP1}$. We have characterized the *pineapple eye* gene and its mutants further to understand how it contributes to proper eye cell number.

MATERIALS AND METHODS

Fly strains: Isolation of the *pie^{EB3}* mutations was described by Baker *et al.* (1992). A similar allele, *pie^{CB6}*, was obtained in the same screen but is no longer extant. Other *pie* alleles were described by Clegg *et al.* (1993). GMRp35 was described by Hay *et al.* (1994); GMRp21 was described by de Nooij and Hariharan (1995); *hid^{WRX+1}* and *hid^{05014}* were described by Grether *et al.* (1995); Df(2L)J2, Df(2L)J27, Df(2L)J39, Df(2L)J77, Df(2L)J106, Df(2L)J16, and Df(2L)J17 were described by Clegg *et al.* (1993); *l(2)54* was described by Sandler (1977); and *mat(2)QM47* was described by Schupbach and Weischaus (1986).

For the mutagenesis, adult males of the genotype *w*; *l(2)k08229/l(2)k10307* were exposed to γ-radiation (4000 rads) and mated with *w;pie^{EB3}*/In(2LR)Gla females. F_1 flies with rough eyes or lacking eye pigmentation were bred where possible to establish stocks putatively mutant for *pie* or deleted for nearby genes. *(2)k08229* and *l(2)k10307* correspond to *P*-element insertions carrying the [w$^+$] gene inserted in chromosome bands 31F1-3 or 31F4-5, respectively (Torok *et al.* 1993).

Histology: Immunochemistry using ELAV, CM1, anti-cyclin B, and anti-cut antibodies was performed as described (Gaul *et al.* 1992; Fu and Noll 1997; Lee *et al.* 2000; Baker and Yu 2001; Yu *et al.* 2002). Sectioned material was prepared as described by Baker *et al.* (1992).

Molecular biology: Growth and selection of bacterial plasmids, cosmids, and bacteriophage were performed according to standard methods (Sambrook *et al.* 1989). For the sequencing of mutant DNA, genomic DNA was prepared from larvae of homozygous *pie^{EB3}* adults or from *pie^{E1-16}*/Df(2L)*J77* third instar larvae selected by absence of the dominant marker *Tubby* present in *pie^{E1-16}*/T(2;3)SM5TM6B and Df(2L)*J77*/T(2;3)SM5TM6B siblings.

RESULTS

The *pie* mutant affects imaginal disc cell survival: As described previously, flies homozygous for the *pie^{EB3}* mutation had rough eyes. Facet size varied from smaller than normal to enlarged, apparently fused facets (Figure 1, A and B). Sections confirmed absence of pigment, cone, and photoreceptor cells (Figure 1, C and D). The pattern of missing cells varied, many ommatidia being normal and no specific cell type being exclusively affected (Baker *et al.* 1992). The adult sections of *pie^{EB3}* homozygotes were essentially indistinguishable from those described for GMRp21, in which arrest of the SMW leads to shortfall of unspecified precursor cells and frequent inability to specify later cell fates (de Nooij and Hariharan 1995).

If *pie^{EB3}* caused arrest of the SMW, we would expect that cyclin B would not accumulate and that mitotic figures would be absent posterior to the morphogenetic furrow, as reported for GMRp21 (Figure 2, A–F). To test this notion, eye discs from *pie^{EB3}* homozygotes were labeled with anti-cyclin B or with basic fuchsin, a stain that reveals mitotic figures. Cyclin B protein accumulates in cells that have progressed through G_1 but not through mitosis. In wild type, 80% of SMW cells divide, mostly in the column 3–5 region posterior to the morphogenetic furrow (Baker and Yu 2001). These cells degrade their cyclin B at mitosis (Evans *et al.* 1983; Knoblich and Lehner 1993). Contrary to the prediction that *pie^{EB3}* arrested the SMW, cyclin B protein was seen to accumulate in a second mitotic wave posterior to the morphogenetic furrow, and mitotic figures were observed in fuchsin-stained preparations (Figure 2, A–F). Fuchsin-stained preparations did reveal a difference in cell death between *pie^{EB3}* and wild-type eye discs, however. Although cell death is rare in wild-type eye discs (Wolff and Ready 1991), abundant apoptotic bodies were evident in *pie^{EB3}* eye discs, both anterior and posterior to the morphogenetic furrow (Figure 2, B and F). Since the rough eye phenotype seen in GMRp21 is thought to be due to a shortfall in the number of cells produced by the SMW, it seemed possible that a similar outcome could result from elevated cell death.

If the *pie^{EB3}* phenotype was caused by excess cell death posterior to the morphogenetic furrow, we predicted that preventing cell death posterior to the morphogenetic furrow would suppress the *pieEB3* phenotype. The GMRp35 transgene was used to suppress cell death. GMRp35 expresses the caspase inhibitor protein baculovirus p35 posterior to the morphogenetic furrow (Hay *et al.* 1994). Basic fuchsin staining confirmed the absence of apoptotic bodies posterior to the morphogenetic furrow in *pie^{EB3}* GMRp35 eye discs, although apoptosis was abundant anterior to the morphogenetic furrow where no p35 protein was expressed (not shown). Adult *pie^{EB3}* GMRp35 flies showed more normal eye morphology than did *pie^{EB3}* homozygotes, although the eyes were still slightly rough and contained some facets of abnormal size (Figure 2, G and H).

These results indicate that the *pie^{EB3}* mutation causes cell death in the eye imaginal disc and that cell death posterior to the morphogenetic furrow contributes to the shortfall of ommatidial cells and to the roughened eye. Because GMRp35 did not suppress the rough eye phenotype completely, it cannot be excluded that *pie^{EB3}* may affect other processes in addition to cell survival. It is also possible, however, that the residual eye rough-

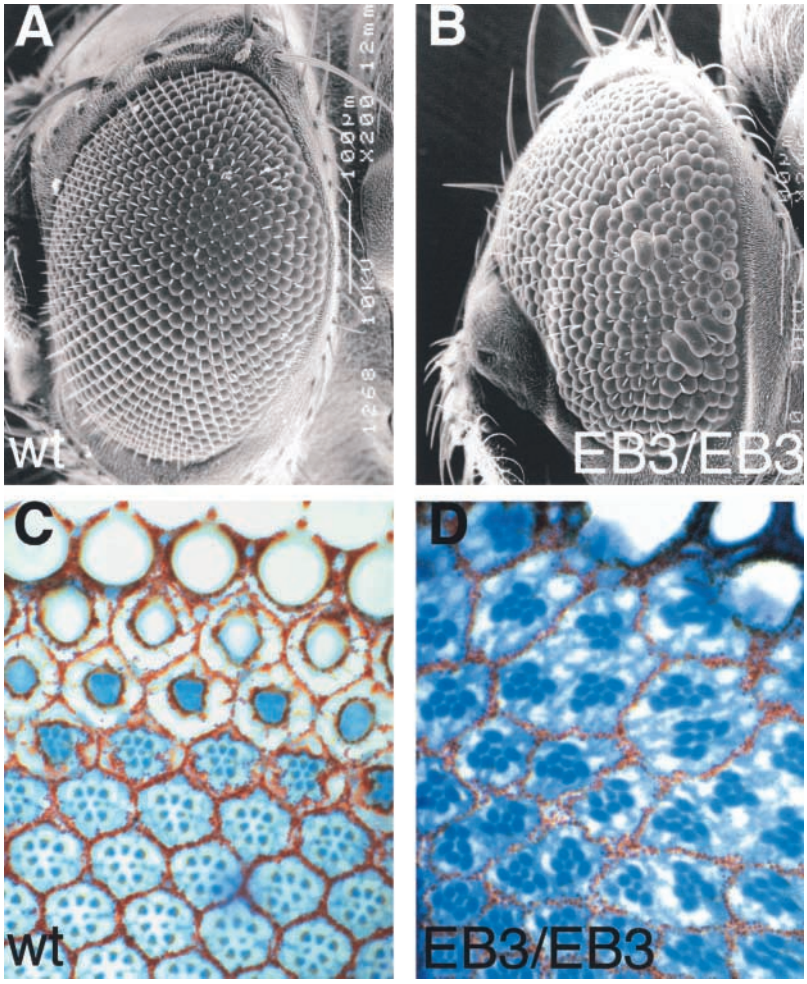

FIGURE 1.—The *pie* mutant phenotype. (A) Scanning electron microscopy shows the regular structure of the wild-type fly eye (anterior to the left). (B) Eyes from pie^{EB3} homozygotes are rough and irregular with variable facet size. Some facets are larger than normal. (C) Section through wild-type eye. The section extends from more distal levels above to more basal levels below. Each ommatidium is similar and surrounded by reddish pigment cells. (D) Section through pie^{EB3} homozygote showing the variable composition of ommatidia. Many ommatidia have too few photoreceptor cells missing. Missing pigment cells result in clusters of photoreceptor cells sharing single enlarged facets. Some ommatidia appear abnormally rotated.

ness is due to cell death triggered within the morphogenetic furrow prior to GMR-driven p35 expression. In addition it should be noted that GMRp35 causes mild eye roughening by itself, due to activity of the p35-insensitive caspase Dronc (YU *et al.* 2002). An attempt was made to assess the effect of earlier blockade of all

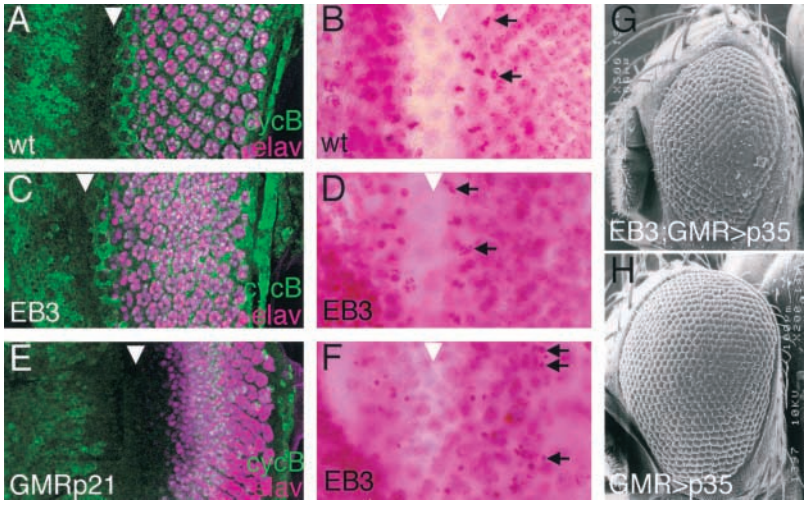

FIGURE 2.—Cell cycle and survival in *pie*. A–F show portions of eye imaginal discs (anterior to the left), labeled either for differentiating photoreceptor cells (ELAV antigen in magenta; A, C, and E) and cyclin B (green; A, C, and E) or with basic fuchsin (B, D, and E). Vertical arrowheads in A–F show the position of column 0. A and B show wild type. Cyclin B labels cells that reenter the cell cycle in the second mitotic wave posterior to the morphogenetic furrow (A). Basic fuchsin labels mitotic figures in the second mitotic wave. (C, D, and F) pie^{EB3} homozygotes. Cyclin B (C) and basic fuchsin (D) identify a second mitotic wave similar to that of wild type. Patterning of ommatidia becomes progressively more abnormal posterior to the morphogenetic furrow, as described previously (BAKER *et al.* 1992). (E) *GMRp21*. Cyclin B reveals normal proliferation anterior to the morphogenetic furrow, but no second mitotic wave posterior to the morphogenetic furrow, quite unlike either wild type or pie^{EB3} (A and C). (F) A more basal focal plane of the same fuchsin-stained pie^{EB3} preparation shown in D reveals many apoptotic bodies (arrows). By contrast dying cells are almost undetectable in wild-type eye discs (not shown). (G) Scanning electron microscopy shows that the adult eye of pie^{EB3} *GMRp35* is much less abnormal than that of pie^{EB3} homozygote (compare Figure 1B). (H) Eyes from *GMRp35* strains are also slightly rough.

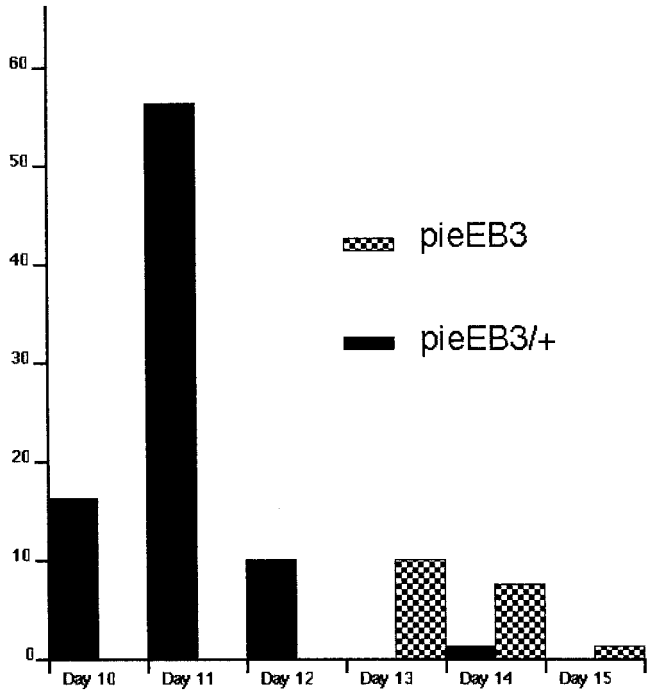

FIGURE 3.—Developmental delay in *pie*. Adult emergence of pie^{EB3} homozygotes and heterozygous $pie^{EB3}/+$ siblings from the same cultures is shown. Flies were reared under uncrowded conditions on rich yeast-glucose food medium to minimize competition for food and resources. The adult pie^{EB3} homozygotes typically emerged 3 days later than controls and comprised 23% of the adult population instead of the expected 50%.

caspases through mutation of *head involution defective* (*hid*), a gene required for all caspase activity and apoptosis during eye development (KURADA and WHITE 1998; YU *et al.* 2002). Since even *trans*-heterozygous $pie^{EB3}/+$; *hid*/+ flies proved inviable, however, the *pie hid* double mutant phenotype could not be examined.

Other imaginal discs were examined to see whether *pie* was required only in eye discs. Basic fuchsin staining identified abnormal excess cell death in wing and leg imaginal discs (not shown but see also Figure 4). In addition, it was noted that pie^{EB3} homozygotes were delayed developmentally (Figure 3). The average (mean) pie^{EB3} homozygote emerged after 13.5 days, 2.5 days later than the average for $pie^{EB3}/+$ controls. In addition, fewer pie^{EB3} homozygotes than predicted were obtained from Mendelian ratios. The pie^{EB3} homozygotes had normal bristle size and morphology (not shown), unlike Minute flies that are developmentally delayed due to reduced translation (MORATA and RIPOLL 1975; LAMBERTSSON 1998) or *diminutive* flies that show reduced cellular growth (JOHNSTON *et al.* 1999). This difference suggests that the delay in pie^{EB3} homozygotes might not be due to deficient translation or growth.

***pie* null alleles are homozygous lethal:** Deficiency chromosomes were used to map the *pie* locus precisely. In a previous study *pie* had been mapped to chromosome interval 32A (BAKER *et al.* 1992), but this proved to be an error. Instead we found that pie^{EB3} failed to complement deficiencies in the 31E region. Specifically, pie^{EB3} failed to complement Df(2L)J2, Df(2L)J27, Df(2L)J39, Df(2L)J77, and Df(2L)J106, but complemented Df(2L)J16 and Df(2L)J17, consistent with location of *pie* in 31E [see CLEGG *et al.* (1993) for details of these deficiencies].

A total of 66,500 flies derived from X-irradiated germ cells (4000 rads) were screened for failure to complement pie^{EB3} to isolate new alleles. Several individuals appearing to carry newly induced *pie* mutations were identified, but in no case did such individuals breed successfully, and the putative new mutations could not be recovered. In addition the pie^{EB3}/deficiency phenotype was semilethal. Those adults that do survive are extremely sickly; the females were invariably sterile and the males bred very poorly. These findings suggested that the pie^{EB3} mutation was hypomorphic and that the *pie* null phenotype might include lethality and/or sterility. To explore this, complementation was tested between pie^{EB3} and representatives of eight lethal complementation groups in the 31E region that, like pie^{EB3}, complemented Df(2L)J16 but not Df(2L)J77 (CLEGG *et al.* 1993). All of these complemented pie^{EB3} except *l(2)31Ek*, indicating that pie^{EB3} was a viable allele of this locus.

Five alleles of *l(2)31Ek* were obtained from existing strains, and all *trans* combinations of these alleles with one another, with pie^{EB3}, and with Df(2L)J77 were examined to identify putative null alleles of the *pie* locus. As noted previously, combinations of *l(2)31Ek* mutations show complex complementation and diverse phenotypes (CLEGG *et al.* 1993). The results are summarized in Table 1. pie^{EB3} is the only homozygous viable allele with an abnormal eye. Multiple *trans*-allelic combinations between lethal alleles are viable with similar rough eyes, however, and the homozygous viable, female sterile allele pie^{QM47} has a rough eye *in trans* to certain other *pie* alleles. Several genotypes, including $pie^{G2\text{-}4}/l(2)54$ and $pie^{E1\text{-}16}/l(2)54$, also exhibit held-up wings and loss of wing margin material.

The complex complementation pattern reported in Table 1 precluded a simple allelic series for *pie* alleles. Two of the alleles behaved most like deficiencies and were studied further. These were $pie^{E1\text{-}16}$, induced by EMS mutagenesis, and $pie^{G2\text{-}4}$, induced by gamma-irradiation.

***pie* null mutations affect cell survival autonomously:** Since both $pie^{E1\text{-}16}$ and $pie^{G2\text{-}4}$ were homozygous lethal, mosaics were studied to determine the effects of *pie* loss of function on imaginal development. Clones of $pie^{E1\text{-}16}$ homozygous cells appeared rougher in adult eyes than clones of pie^{EB3} did (Figure 4, A and B). Imaginal disc clones were examined by confocal microscopy after labeling with antibodies against Elav, to detect differentiating photoreceptor cells, or against Cut, to detect nonneuronal cone cells (Figure 4, C–F). Whereas clones of

TABLE 1

Heteroallelic combinations of *pie* mutations

	J77	E1-16	G2-4	E1-2	EB3	QM47	H113	*l(2)54*
J77	L	L	L	L	R, D, I	I	L	mR, I
E1-16		L	L	L	R, D, I	R, D	L	R
G2-4			L	L	R, D, I	R, D, I	L	R
E1-2				L	R	R, I	L	R
EB3					R, D, I	mR, I	R	wt
QM47						L	mR	R
H113							L	L
l(2)54								L

L, lethal; R, roughened eye; mR, mildly roughened eye; D, developmental delay; I, infertile (or nearly so); F, fertile; wt, wild type. Fertility was not examined for some viable combinations.

pie^{EB3} developed almost normally (Figure 4, C and E), $pie^{E1\text{-}16}$ clones contained smaller ommatidial clusters showing a variable shortfall in photoreceptor and cone cell differentiation (Figure 4, D and F).

The development of $pie^{E1\text{-}16}$ clones resembled that of pie^{EB3} homozygotes, suggesting that $pie^{E1\text{-}16}$ also caused imaginal disc cell death. To test this, $pie^{E1\text{-}16}$ clones were labeled with an antibody that recognizes activated caspases. Caspases were activated in many $pie^{E1\text{-}16}$ homozygous cells in eye disc and wing disc clones and the morphology of the labeled cells supported the hypothesis that they were apoptotic (Figure 4, H and J). Not all homozygous $pie^{E1\text{-}16}$ cells label for activated caspase at any given time. Apoptotic cells were evenly distributed through the clones, not obviously correlated with distance to wild-type cells outside the clone, consistent with an autonomous effect on cell survival (Figure 4, H and J).

The development of pie^{EB3} clones was less abnormal than that of pie^{EB3} homozygotes, suggesting that the pie^{EB3} mutation might act nonautonomously. To test this, pie^{EB3} clones were labeled with an antibody that recognizes activated caspases. pie^{EB3} clones showed abundant cell death, similar to pie^{EB3} homozygotes, suggesting that pie^{EB3} affects cell survival autonomously (Figure 4, G and I). As for $pie^{E1\text{-}16}$, apoptotic cells were distributed evenly through pie^{EB3} clones. We suggest that in mosaics, normal cells from outside pie^{EB3} clones are recruited to cell fates in place of pie^{EB3} homozygous cells that have died, permitting more normal development of pie^{EB3} clones than is possible for pie^{EB3} homozygotes.

Molecular identification of the *pie* gene: As a first step toward locating the *pie* gene, genomic cosmid clones from the 31E region were obtained (Siden-Kiamos *et al.* 1990) and restriction mapping and Southern blotting were used to prepare a map of the 31E region (Figure 5A). PCR primers were based on the sequence of the *da* gene (which maps left of *pie* genetically) within clone 100A9. Reduced Southern blot signals in heterozygotes located the proximal break of Df(2L)J77 within clone 192F1. Df(2L)J77 is null for *pie*, placing the *pie* gene within a genomic region of ~70 kb (Figure 5A).

Since radiation-induced mutations are often associated with DNA lesions detectable by Southern blotting, DNA from the gamma-induced mutation $pie^{G2\text{-}4}$ was compared with control DNA across the critical region. A single polymorphism was detected 29 kb to the right of *da*. Southern blots with multiple enzymes mapped a breakpoint that was not present in the unmutagenized progenitor strain to a 300-bp segment defined by *Eco*RI and *Bam*HI restriction sites (Figure 5, A and B). Since no deletion or duplication was indicated, the Southern analysis predicted that $pie^{G2\text{-}4}$ was associated with an inversion. Polytene chromosomes were examined to test this. The $pie^{G2\text{-}4}$ chromosome was found to contain a cytologically visible inversion between chromosome regions 31E and 32A (not shown). These findings were consistent with the model that gamma-irradiation induced a chromosome inversion breaking within the *pie* gene to generate the $pie^{G2\text{-}4}$ allele.

To identify genes affected by the $pie^{G2\text{-}4}$ inversion breakpoint in 31E, genomic *Bam*HI fragments around the breakpoint (8.3 kb in total) were used to probe a cDNA library derived from imaginal disc RNA (gift of A. Cowman and G. M. Rubin). Inserts from positive clones were characterized by restriction map and cross-hybridization and fell into three discrete classes, indicating three transcription units in the $pie^{G2\text{-}4}$ region (Figure 5B). The largest clone was sequenced for each of the three cDNA classes, and corresponding genomic DNA was also sequenced to establish the intron-exon structure. The leftmost clone contained a 3242-bp cDNA predicted to encode a novel kinesin-like protein (GenBank accession no. AF247500). The second clone contained an 1148-bp cDNA predicted to encode a replication factor C protein (GenBank accession no. AF247499). The most centromeric clone contained an 1852-bp cDNA encoding a novel protein (GenBank accession no. AF247501). The G2-4 breakpoint mapped toward the 3′ end of this transcript (Figure 5B).

We predicted that if the centromeric 1852-bp cDNA corresponded to the *pie* gene, the open reading frame might be altered in point mutants. Genomic DNA was

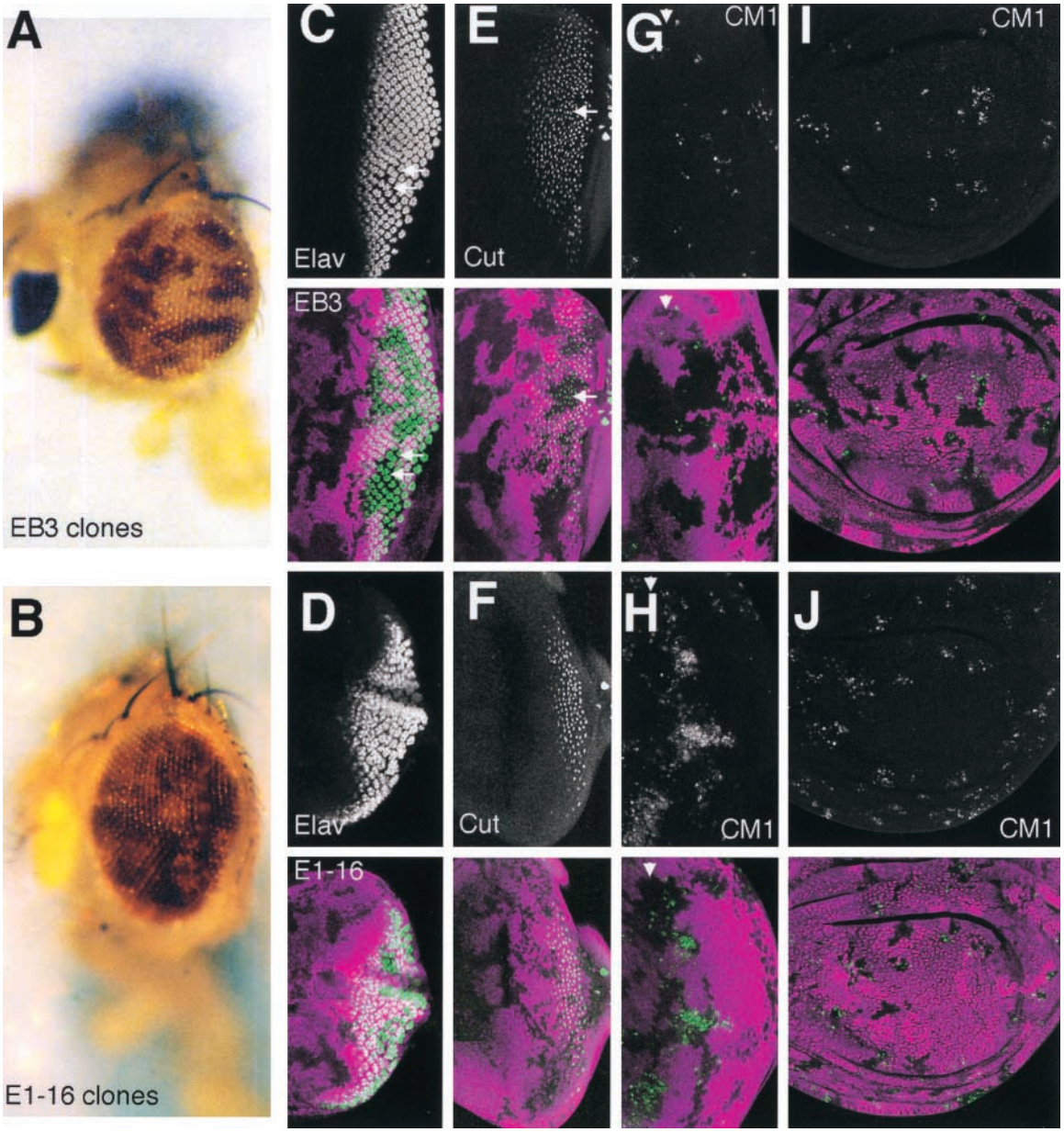

FIGURE 4.—Cell death in *pie* mutant clones. (A) Head containing pie^{EB3} homozygous clones (unpigmented) generated by eyFlp-mediated mitotic recombination. Homozygous mutant tissue occupies as much of the eye as the darkly pigmented twin spots and shows almost normal morphology, unlike the rough appearance of entirely mutant pie^{EB3} eyes (compare Figure 1B). (B) Head containing $pie^{E1\text{-}16}$ homozygous clones (unpigmented) generated by eyFlp-mediated mitotic recombination. Homozygous clones occupy little of the adult eye, which has a roughened appearance. C–F show differentiation in eye discs containing clones of cells homozygous for pie^{EB3} (C and E) or $pie^{E1\text{-}16}$ (D and F) mutations. ELAV labeling of differentiating photoreceptor cells in C and D shows neighboring ommatidial clusters touching due to lack of intervening nonneural cells (arrows). The defect is less extreme in pie^{EB3} clones than in pie^{EB3} homozygotes, however (compare C with Figure 2C). Cone cells detected by cut expression are also abnormally arranged within mutant clones (E, pie^{EB3}; F, $pie^{E1\text{-}16}$). G–J show imaginal discs labeled for apoptotic cells containing activated caspases. G and H show eye imaginal discs containing clones of cells homozygous for pie^{EB3} (G) or $pie^{E1\text{-}16}$ (H). I and J show wing imaginal discs containing clones of cells homozygous for pie^{EB3} (I) or $pie^{E1\text{-}16}$ (J). Apoptotic cells are seen within mutant clones both anterior and posterior to the morphogenetic furrow in the eye disc and in wing discs. Cell death is less abundant in pie^{EB3} clones than in $pie^{E1\text{-}16}$ clones. pie^{EB3} clones are also larger than $pie^{E1\text{-}16}$ clones. Note that cell death occurs fairly evenly through mutant clones, does not seem concentrated in particular disc regions, and is neither more nor less prevalent near clonal boundaries with wild-type cells.

sequenced from the EMS-induced pie^{EB3} and $pie^{E1\text{-}16}$ alleles and compared with the unmutagenized control chromosomes to assess this. Whereas neither the kinesin-like gene nor the RFC gene was altered in these mutations, the third gene was altered in both. The pie^{EB3} chromosome contained a C-to-T transition at position

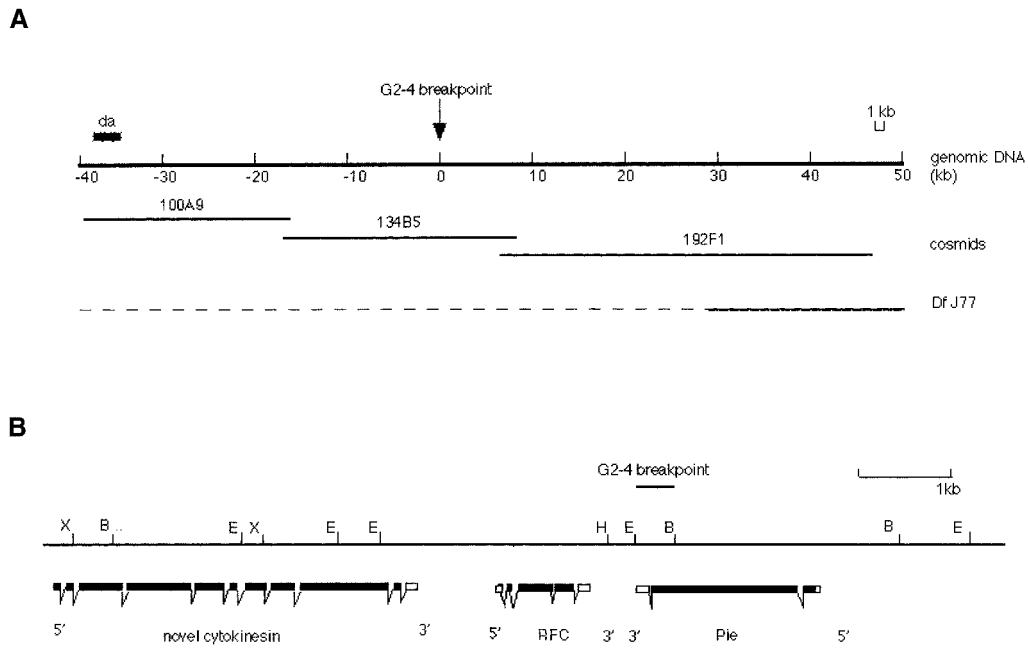

C

```
MEDNKELQCL ICKYSDTDDL VFGEWMIVRN LQVHYFCLLL STHLPQRGGD SSGILGFLLR
DIREEAAAAE KRKCWYCNKI GASLQCDRCR SLFHLKCGLE NRAVFEFCGQ YKSYCYKCRP
MDDYKRQLQS KPPRNATCPI CFSSIYKVEL HCVVYGDCCR LGFAHKKCMR QYALTSGYYL
RCIWCRSERF RDSIRLQSVF VPDRDATWEK QRNAYRELHE RNLKCDQPNC LCPSGRTYNR
LSWVILCCSS CAATSAHLKC LVGALRLPKK RERTDFKCSM CLDVERRIAE GPARTTEETN
ADGDNQVDGS FYVQKLGPDA ATRSLTQTPV FSEEDESERS SNITVIFSQP KSNATSERLS
LSPPQEEMIV EIPDSPEASP KTSIDENHSP QPIARRDISD SPQPIAASEI PDSPQPTAAS
EIPDLPQTTA INVNPELTQQ TALNTIPHSP QPEASFPTQL VSQTFDSPQP QEQAVAEAPN
SPSLPKEDPN TLLVLKSGFQ CPGEPFFYLV IYEFEHGTCM GECIGTCVLR FKEDDPRIQD
TSQAALERVK ITPDDVWCRS EDRGIFEHIE KFHEWYRSEG FS
```

FIGURE 5.—Genomic organization of the *pie* region. (A) Three cosmid clones from the 31E region were determined by restriction mapping and cross-hybridization to cover ~90 kb of genomic DNA including the *daughterless* gene and the proximal breakpoint of Df(2L)J77. The position of the inversion breakpoint associated with $pie^{G2\text{-}4}$ is shown and assigned as the origin on the arbitrary scale. (B) More detailed map of the $pie^{G2\text{-}4}$ breakpoint region including genomic organization of three transcription units identified by screening an imaginal disc cDNA library. The breakpoint maps within 300 bp close to the 3′ end of the *pie* transcript. Coding regions are indicated by solid shading of the exon bars. (C) Amino acid sequence predicted by the *pie* open reading frame. The allele $pie^{E1\text{-}16}$ is frameshifted at Asp203 (boldface, underlined). The allele pie^{EB3} replaces Gln391 with a stop codon (boldface, underlined). A consensus defined for molybdopterin binding, [GA]-X(3)-[KRNQHT]-X(11,14)-[LIVMFYWS]-X(8)-[LIVMF]-X-C-X(2)-[DEN]-R-X(2)-[DE] (WOOTON *et al.* 1991), is matched by amino acids Gly156, Arg160, Leu174, Ile183, Cys185, Glu188, Arg189, and Asp192 of the predicted PIE protein.

1213 compared to the cDNA sequence, substituting a TAG stop codon for the CAG codon for Gln391 of the predicted protein (Figure 5C). The $pie^{E1\text{-}16}$ chromosome contained a 13-bp deletion corresponding to nucleotides 644–656 of the cDNA, predicting the substitution of a novel sequence of 16 amino acids followed by a termination codon for Asp203 (Figure 5C). Taken together with the rearranged transcription unit in the $pie^{G2\text{-}4}$ allele, these results confirm the identity of this novel open reading frame with the *pie* gene. Truncation of the $pie^{E1\text{-}16}$ product earlier than that of pie^{EB3} may explain why pie^{EB3} is hypomorphic compared to $pie^{E1\text{-}16}$ and $pie^{G2\text{-}4}$.

The *pie* gene sequence predicts a protein of 582 amino acids that lacks apparent secretory signal sequences, potential transmembrane domains, or recognized conserved domains (Figure 5C). Since it also lacks apparent nuclear localization or mitochondrial import sequences, it is possible that *pie* encodes a cytoplasmic protein. Inspection of the sequence suggests that the PIE protein can be viewed as containing two domains (Figure 5C). Cysteine is unusually common among amino acids 9–281 (27 of these 273 codons encoded cysteine). Proline is unusually common among amino acids 291–505 (31 of these 215 codons encoded proline).

Database searches identified several predicted genes of unknown function from human, mice, and mosquitoes that contained regions highly similar to the Cys-rich region of PIE. Figure 6 shows an alignment of seven related sequences and the Cys-rich domain from PIE. All but one of these domains show 30–35% amino acid identity with PIE and ~50% similarity. This very high degree of similarity speaks to a highly conserved structure and molecular function. No one of these seven

```
AF247501(PIE)                          MEDNKE LQCLICKYSD TDDLVFG--- EWMIVR--NL QVHYFCLLLS THLPQRG-GD
EAA07617                                  MA KVCFLCKSSE DDELLFG--- --KFYTKWRL SVHYYCLLLS SNLVQNGVND
NM134530                                  MV QICVLCLSGE RDELIFG--- --TVHVEGNM MVHRNCLYLS SNLIQRG-EK
AB037554                        M NESKPGDSQN LACVFCRKHD DCPNKYG--- EKKTKEKWNL TVHYYCLLMS SGIWQRGKEE
XM_126910                       M NENKPDNSQS LACVFCRKND DCPNKYG--- EKKTYEKWNF SVHYYCLLMS SGIWQRGKEE
BC02202   MKTVKEKKEC QRLRKSAKTR RVTQRKPSSG PVCWLCLREP GDPEKLG--- E--FLQKDNI SVHYFCLILS SKLPQRGQSN
NM027949  MKTLKEKNKH PRLRKTIRTK KVTQRKLSSS PVCLLCLQEP GDPEKLG--- E--FLQKDNL CVHYFCLILS SRLPQKGQPN
T46480
AF151060                                     CLLALREP GDPEKLG--- E--FLQKDNI SVHYFCLILS SKLPQR
EAA00707                                     CDICLLNE NNPLRYGEFV EKVYKTQRKI RAHYFCLLSG TNIPQNG-ST

AF247501  SSGILGFLLR DIREEAAAAE KRKCWYCNKI GASLQC--DR CRSLFHLKCG LENRAVFEFC GQYKSYCYKC RPMDDYKRQL
EAA07617  TVGIFGFLEQ DIRKENERTK KCRCYICKEM HANVSCCSKK CLRTFHTVCG IKNRCLSHYT DTFQSWCASH IPVERDA---
NM1345030 KLSIMNFLKE DIEAEVNRCR LLKCCYCRRL GANIWCCKSG CRRTFHTKCG VDNLAQNQFC DTYNSFCHQH VLVPRNR---
ABO37554  E-GVYGFLIE DIRKEVNRAS KLKCCVCKKN GASIGCVAPR CKRSYHFPCG LQRECIFQFT GNFASFCWDH RPVQIIT---
XM_126910 E-GVYGFLIE DIRKEVQRAS KLKCTVCKKN GASIGCVVPT CKRSYHLPCG LQKECIFQFT DNFASFCWKH RPVQAIT---
BC02202   R-GFHGFLPE DIKKEAARAS RKICFVCKKK GAAINCQKDQ CLRNFHLPCG QERGCLSQFF GEYKSFCDKH RPTQNIQ---
NM027949  R-GLHGFMPE DIKREAVRAS KKICFVCKKK GAAIRCQNDQ CVQNFHLPCG QERGCLSQFF GEYKSYCRKH RPTQNIH---
T46480                       RAS RKICFVCKKK GAAINCQKDQ CLRNFHLPCG QERGCLSQFF GEYKSFCDKH RPTQNIQ---
AF151060        FLPE DIKKEAARAS RKICFVCKKK GAAINCQKDQ CLRNFHLPCG QERGCLSQFF GEYKSFCDKH RPTQNIQ---
EAA00707  PAGIAGFKIS DVLSSYAEYR EKQCYYCRHP SAPVECAQAG CGRRYHYICG YNNSCVTQFV GEFRSYCDQH LP----EGCR

AF247501  QSKPPRNATC PICFSSIY-- --K-VELHCV VYGDC---CR LGFAHKKCMR QYALTSG-YY LRCIWCRS-E RF-RDSIRLQ
EAA07617  QPHTAEE-PC SICYDEM--- GQ--YDRITS IRAPC---CR NGWFHQRCVA QYAQSAG-YF FKCPLCNNED TFLPEIPRR-
NM1345030 PVFKNDE-EC LLCAEDVVAK GER-FSVVTC LYAPC---CR NGWFHRRCLQ RYANSSG-YF FKCPLCNNTD VF-RRVAYM-
ABO37554  SNNYRESLPC TICLEFI--- -EP-IPSYNI LRSPC---CK NAWFHRDCLQ VQAINAGVFF FRCTICNNSD IFQKEMLRM-
XM_126910 SNKYSSSLPC TICLEFV--- -EP-IPTYNI LQSPC---CK NAWFHRDCLQ VQAINAGVFF FRCTLCNNTD IFQKEMLRM-
BC02202   HGHVGEE-SC ILCCEDL--- -SQ-QSVENI -QSPC---CS QAIYHRKCIQ KYAHTSAKHF FKCPQCNNRK EFPQEMLRM-
NM027949  QGSLGEE-SC VLCCENL--- -SR-TSVENI -QSPC---CS QAIYHRKCIQ KYAHTSAKHF FKCPQCNNRE EFPQEMLRM-
T46480    HGHVGEE-SC ILCCEDL--- -SQ-QSVENI -QSPC---CS QAIYHRKCIQ KYAHTSAKHF FKCPQCNNRK EFPQEMLRM-
AF151060  HGHVGEE-SC ILCCEDL--- -SQ-QSVENI -QSPC---CS QAIYHRKCIQ KYAHTSAKHF FKCPQCNNRK SFLKKC
EAA00707  VPVTTKGRRC SICFEDLPQV TEPDYNPLSI VRTHCDSECP PGLLHRECVQ RFAYTSG-YN FKCPLCWN-K AFRVHAAEV-

AF247501  SVFVPDRDAT WEKQRNAYRE LHERNLKCDQ PNCLCPSGRT YNRLS----- --WVILCCSS CA-ATSAHLK CLVGALRLPK
EAA07617  GVFVPERDAA WELEPNAFQE QLVRPTACDS EDCKCEQGRS -------VDS HEWRLVICGS CG-STCRHRQ CMEATPELTR
NM1345030 GIAVLDQDAS WETEPDAFAG QYRRDVNCTA ALCVAVSGRA -------DTS A--MLLYCTS CG-ANPSHYL C---TLKTLQ
ABO37554  GIHIPEKDAS WELEENAYQE LLQHYERCDV RRCRCKEGRD YNAPD----- SKWEIKRCQC CG-SSGTHLA CSSLRSW-EQ
XM_126910 GIHIPEKDAS WELEENAYQE LLQSHDRCDI RRCHCKKGRD YNEPNRFPKG PQTPISQLY
BC02202   GIHIPDRDAA WELEPGAFSD LYQRYQHCDA PICLYEQGRD -----SFEDE GRWCLILCAT CG-SHGTHRD CSSLRPN-SK
NM027949  GIHIPDRDAA WELEPGAFSE LYQRYRHCDA PICLYEQGRD -----SFEDE GRWRLILCAT CG-SHGTHRD CSSLRPN-SK
T46480    GIHIPDR
AF151060
EAA00707  GIFIPQRESA WEREPGAFKD LHKR--KCTA VDCKVGNGRN AANQLVGCKV CGGQLMHRQC CGVSDADDYL CSGC

AF247501  KRERTDFKCS MC
EAA07617  A-----YVCQ LCRPI
NM1345030 N-----YVCK VCSAV
ABO37554  N-----WECL ECRGI
BC02202   K-----WECE ECSPA
NM027949  K-----WECN ECLPA
```

FIGURE 6.—Comparison of PIE to other genes. BLAST searches detect a number of other predicted genes sharing cysteine-rich domains to the amino-terminal portion of the predicted PIE protein (AF247501). Shown are alignments between amino acids 1–281 from PIE and portions of predicted proteins from *Anopheles gambiae* (EAA07617 and EAA00707), *D. melanogaster* (NM1345030 corresponding to CG9576), *Mus musculus* (XM_126910 and NM027949), and *Homo sapiens* (AB037554, BC02202, and T46480). Amino acids identical with the corresponding PIE amino acid are shown in magenta; conservative substitutions are shown in green. AB037554 and XM_126910 are likely human and mouse orthologs of one another, as are BC02202 and NM027949, but evolutionary relationships among the other sequences are less clear (not shown).

sequences appears significantly more closely related to PIE, and which if any of the vertebrate sequences might be a *pie* ortholog is not apparent. Although the arrangement of cysteines is strongly conserved, there are several examples of nonconserved cysteines, and Cys118 from PIE is replaced by histidine in all the other sequences. This observation, along with the lack of apparent transmembrane or signal sequences and the presence of several perfectly conserved histidines, suggests the PIE protein might be involved in metal binding. In addition, the PIE sequence contains the consensus for molybdopterin binding (Figure 5C; Interpro IPR000572; Prosite PS00559). Molybdopterin is the molybdenum cofactor for all molybdenum-containing enzymes except one

(Wootton *et al.* 1991). None of the other proteins match the molybdopterin-binding consensus, and we therefore suspect that the consensus in PIE may be fortuitous.

Many Pro-rich protein sequences were found by similarity searches with the Pro-rich domain of PIE but none appeared to resemble PIE specifically or also to contain the Cys-rich PIE domain. However, the second Drosophila gene identified as sharing the PIE Cys-rich domain (Figure 6), which corresponds to predicted gene CG9576 (Adams *et al.* 2000), resembles PIE in also containing a carboxyl region rich in Pro, Ser, and acidic residues, although these regions from PIE and CG9576 cannot be satisfactorily aligned (not shown).

Attempts to express portions of the PIE protein as bacterial fusion proteins were largely unsuccessful; only a fusion of the carboxy-terminal 67 amino acids fused to the carboxyl terminus of glutathione *S*-transferase has been obtained. Immunization with this protein produced mouse antisera that were specific for the PIE-specific portion of the fusion protein on Western blots, but could not detect endogenous PIE protein products by Western blotting or immunostaining of Drosophila tissues or cells. The *pie* gene must be expressed in imaginal disc cells, however, since it was required there cell autonomously.

DISCUSSION

In this article we used the adult eye phenotype associated with defective cell number to identify a candidate gene for cell number regulation and have shown that this *pineapple eye* gene encodes a putative cytoplasmic protein required for proper cell survival. Unlike some cell lethal mutations, *pie* mutations are not absolutely inviable, but instead predispose cells in imaginal discs to a high rate of apoptosis. Apoptosis is identifiable by activation of endogenous caspases and preventable by retinal expression of the caspase inhibitor p35. Within imaginal discs of *pie* mutants, apoptosis occurred indiscriminately at many locations, and no obvious spatial pattern of sensitivity was observed. We focused on eye and wing imaginal discs but noticed cell death in other imaginal discs also (data not shown). It is intriguing that the main function of *pie* should seem to be reducing the rate of apoptosis, but as yet we have no clue about the molecular or biochemical function of the protein product. Nevertheless, the *pie* gene contains a domain of ~270 amino acids with striking homology throughout the animal kingdom. So far all these genes are of unknown biochemical function, although we suspect that this may be a metal-binding domain.

The *pie* mutant phenotype illustrates the distinct consequences of cell death at different developmental stages. Retinal cell death posterior to the morphogenetic furrow leads to a shortfall in retinal precursor cells and so to defects in the ommatidial structure of the mature retina. These defects resemble those seen when the second mitotic wave is blocked. This emphasizes the importance of adequate cell number for retinal development and confirms that the second mitotic wave is important for providing adequate precursor cells (de Nooij and Hariharan 1995). The *pie* phenotype further indicates that retinal cells cannot be replaced after the second mitotic wave. Even though *pie* mutants have seemingly normal cell proliferation, cells lost posterior to the morphogenetic furrow are not replaced by compensatory cell divisions. An indication of this fact also came from previous findings that X-ray damage incidental to induction of mitotic recombination was associated with defects in ommatidial structure among cells posterior to the morphogenetic furrow at the time of irradiation, but irradiation earlier had little effect on retinal structure (Becker 1957).

Remarkably, the retina is the exception in exhibiting morphological defects as a consequence of high rates of cell death (along with the wing margin, which is also abnormal in certain allelic combinations). Developmental delay seems to be the main effect of cell death in other tissues, without obvious morphological consequences. Previous studies of imaginal disc damage indicate that imaginal discs need to attain a critical size to trigger metamorphosis (Russell 1974; Simpson and Schneiderman 1975). More accurately, since removing entire imaginal discs has no effect on developmental timing, presence of immature or growing imaginal discs must inhibit metamorphosis (Simpson *et al.* 1980; Szabad and Bryant 1982). The *pie* phenotype suggests that the critical threshold beyond which imaginal discs cease preventing metamorphosis must be cell number or a property dependent on cell number, such as tissue mass or range of pattern.

The lack of morphological consequences of cell death in the *pie* mutant also contrasts with two other phenomena associated with cell death, namely pattern duplication and cell competition. Pattern anomalies such as leg duplications and triplications have not been seen in *pie* mutants although they are commonplace when clones of conditionally lethal cells die [reviewed in Meinhardt (1983)]. Such duplications are thought to result from inappropriate apposition of distinct cell populations on death of intervening cells, if the distinct cell populations interact to induce a new organizing region in the imaginal disc (Meinhardt 1983). One possibility is that apoptotic cell death in *pie* removes cells in a different way from the uncharacterized death mechanisms of conditional-lethal cells. Alternatively, we speculate that stochastic apoptosis in *pie* mutants occurs in a salt-and-pepper fashion so that sufficient cells always survive to buffer spatially distinct cell populations.

Cell competition is another phenomenon associated with cell death. Cell competition occurs when cell populations with different growth rates are apposed within the same compartment, such as occurs when clones of

genetically wild-type cells are induced by mitotic recombination in a Minute heterozygous background (Morata and Ripoll 1975). Doubling of the faster growing cells is accelerated at the expense of the slower genotype, which can actually be eliminated from the compartment where it would have flourished had wild-type cells not been introduced. Recently several studies have indicated that apoptosis plays a significant role in eliminating the slower growing, competed cells (Neufeld *et al.* 1998; Moreno *et al.* 2002). By contrast, clones of cells homozygous for *pie* mutations survive late into larval and even adult life, despite exhibiting much higher rates of apoptosis than surrounding cells. The apparent failure of *pie* homozygous clones to suffer from cell competition raises the possibility that apoptosis is not sufficient for cell competition to occur or that apoptosis in cell competition has particular spatial or biochemical properties that are not shared by apoptosis due to other causes.

In summary, we interpret two aspects of the *pie* phenotype to represent distinct consequences of the underlying cell death and to reflect changing importance of proper cell number during imaginal disc development. During the bulk of larval life the main role of increasing imaginal disc cell number is to provide adequate material for adult tissues. Once this is attained and adult differentiation begins, organs such as the adult retina must maintain precise cell numbers because almost every cell is specified for a particular fate and cannot be replaced if lost. In other organs, such as legs or wings, the most cells take relatively uniform epidermal fates and can substitute for one another with little consequence. These changing roles may in part justify temporal differences in cell cycle control, in which signals such as EGFR and Hh play essential cell cycle and survival roles in differentiating eye discs that differ from their roles during prior imaginal disc growth (Baker and Yu 2001; Duman-Scheel *et al.* 2002).

We thank our colleagues and I. Hariharan and K. Moses for reading the manuscript. We are grateful to R. Mottus, T. Grigliatti, and T. Schupbach for Drosophila strains; I. Siden-Kiamos for cosmids; G. Rubin for cDNA libraries; and P. O'Farrell, the Developmental Studies Hybridoma Bank at the University of Iowa, A. Srinivasan, and Idun Pharmaceuticals for antibodies. This work was supported by grants from the Howard Hughes Medical Institute Research Resources Program for Medical Schools, the U.S. Army Medical Research and Material Command, and the National Institutes of Health (GM-61230).

LITERATURE CITED

Adams, M. D., S. E. Celniker, R. A. Holt, C. A. Evans, J. D. Gocayne *et al.*, 2000 The genome sequence of *Drosophila melanogaster*. Science **287:** 2185–2195.

Baker, N. E., 2001 Proliferation, survival and death in the *Drosophila* eye. Semin. Cell Dev. Biol. **12:** 499–507.

Baker, N. E., and S.-Y. Yu, 2001 The EGF receptor defines domains of cell cycle progression and survival to regulate cell number in the developing *Drosophila* eye. Cell **104:** 699–708.

Baker, N. E., K. Moses, D. Nakahara, M. C. Ellis, R. W. Carthew *et al.*, 1992 Mutations on the second chromosome affecting the *Drosophila* eye. J. Neurogenet. **8:** 85–100.

Becker, H. J., 1957 Uber Rontgenmosaikflecken und Defektmutationen am Auge von *Drosophila* und die Entwicklungsphysiologue des Auges. Z. Indukt. Abstammungs. Vererbungsl. **88:** 333–373.

Clegg, N. J., I. P. Whitehead, J. K. Brock, D. A. Sinclair, R. Mottus *et al.*, 1993 A cytogenetic analysis of chromosome region 31 of *Drosophila melanogaster*. Genetics **134:** 221–230.

de Nooij, J. C., and I. K. Hariharan, 1995 Uncoupling cell fate determination from patterned cell division in the *Drosophila* eye. Science **270:** 983–985.

Duman-Scheel, M., L. Weng, S. Xin and W. Du, 2002 Hedgehog regulates cell growth and proliferation by inducing Cyclin D and Cyclin E. Nature **417:** 299–304.

Edgar, B. A., J. Britton, A. F. de la Cruz, L. A. Johnston, D. Lehman *et al.*, 2001 Pattern- and growth-linked cell cycles in *Drosophila* development. Novartis Found. Symp. **237:** 36–42.

Evans, T., E. T. Rosenthal, J. Youngblom and T. Hunt, 1983 Cyclin: a protein specified by maternal mRNA in sea urchin eggs that is destroyed at each cleavage division. Cell **33:** 389–396.

Fu, W., and M. Noll, 1997 The Pax2 homolog *sparkling* is required for development of cone and pigment cells in the *Drosophila* eye. Genes Dev. **11:** 2066–2078.

Gaul, U., G. Mardon and G. M. Rubin, 1992 A putative Ras GTPase activating protein acts as a negative regulator of signaling by the sevenless receptor tyrosine kinase. Cell **68:** 1007–1019.

Grether, M. E., J. M. Abrams, J. Agapite, K. White and H. Steller, 1995 The *head involution defective* gene of *Drosophila melanogaster* functions in programmed cell death. Genes Dev. **9:** 1694–1708.

Hay, B. A., T. Wolff and G. M. Rubin, 1994 Expression of baculovirus P35 prevents cell death in *Drosophila*. Development **120:** 2121–2129.

Johnston, L. A., and P. Gallant, 2002 Control of growth and organ size in *Drosophila*. BioEssays **24:** 54–64.

Johnston, L. A., D. A. Prober, B. A. Edgar, R. N. Eisenman and P. Gallant, 1999 *Drosophila myc* regulates cellular growth during development. Cell **98:** 779–790.

Knoblich, J. A., and C. F. Lehner, 1993 Synergistic action of *Drosophila* cyclin A and B during the G_2-M transition. EMBO J. **12:** 65–74.

Kurada, P., and K. White, 1998 Ras promotes cell survival in *Drosophila* by downregulating *hid* expression. Cell **95:** 319–329.

Lambertsson, A., 1998 The *Minute* genes in *Drosophila* and their molecular functions. Adv. Genet. **38:** 69–134.

Lee, E.-C., S.-Y. Yu and N. E. Baker, 2000 The SCABROUS protein can act as an extracellular antagonist of Notch signaling in the *Drosophila* wing. Curr. Biol. **10:** 931–934.

Meinhardt, H., 1983 Cell determination boundaries as organising regions for secondary embryonic fields. Dev. Biol. **96:** 375–385.

Morata, G., and P. Ripoll, 1975 Minutes: mutants of *Drosophila* autonomously affecting cell division rate. Dev. Biol. **42:** 211–221.

Moreno, E., K. Basler and G. Morata, 2002 Cells compete for decapentaplegic survival factor to prevent apoptosis in *Drosophila* wing development. Nature **416:** 755–759.

Neufeld, T. P., and I. K. Hariharan, 2002 Regulation of growth and cell proliferation in eye development, pp. 107–133 in *Drosophila Eye Development*, edited by K. Moses. Springer Verlag, New York.

Neufeld, T. P., A. F. de la Cruz, L. A. Johnston and B. A. Edgar, 1998 Coordination of growth and cell division in the *Drosophila* wing. Cell **93:** 1183–1193.

Oldham, S., R. Bohni, H. Stocker, W. Brogiolo and E. Hafen, 2000 Genetic control of size in Drosophila. Philos. Trans. R. Soc. Lond. B **355:** 945–952.

Russell, M. A., 1974 Pattern formation in the imaginal discs of a temperature-sensitive cell-lethal mutant of *Drosophila melanogaster*. Dev. Biol. **40:** 24–39.

Sambrook, J., E. F. Fritsch and T. Maniatis, 1989 *Molecular Cloning: A Laboratory Manual*, Ed. 2. Cold Spring Harbor Laboratory Press, Cold Spring Harbor, NY.

Sandler, L., 1977 Evidence for a set of closely linked autosomal genes that interact with sex chromosome heterochromatin in *Drosophila melanogaster*. Genetics **86:** 567–582.

Schupbach, G., and E. Weischaus, 1986 Maternal-effect mutations altering the anterior-posterior pattern of the *Drosophila* embryo. Roux's Arch. Dev. Biol. **195:** 302–317.

Siden-Kiamos, I., R. D. Saunders, L. Spanos, T. Majerus, J. Treanear *et al.*, 1990 Towards a physical map of the *Drosophila melano-*

gaster genome: mapping of cosmid clones within defined genomic regions. Nucleic Acids Res. **18:** 6261–6270.

Simpson, P., and H. A. Schneiderman, 1975 Isolation of temperature-sensitive mutations blocking clone development in *Drosophila melanogaster*, and the effects of a temperature-sensitive cell lethal mutation on pattern formation in imaginal discs. Roux's Arch. Dev. Biol. **178:** 247–275.

Simpson, P., P. Berreur and J. Berreur-Bonnenfant, 1980 The initiation of pupariation in *Drosophila*: dependence on growth of the imaginal discs. J. Embryol. Exp. Morphol. **57:** 155–165.

Szabad, J., and P. J. Bryant, 1982 The mode of action of "discless" mutations in *Drosophila melanogaster*. Dev. Biol. **93:** 240–256.

Torok, T., G. Tick, M. Alvarado and I. Kiss, 1993 *P-LacW* insertional mutagenesis on the second chromosome of *Drosophila melanogaster*: isolation of lethals with different overgrowth phenotypes. Genetics **135:** 71–80.

Wolff, T., and D. F. Ready, 1991 Cell death in normal and rough eye mutants of *Drosophila*. Development **113:** 825–839.

Wolff, T., and D. F. Ready, 1993 Pattern formation in the *Drosophila* retina, pp. 1277–1326 in *The Development of Drosophila melanogaster*, edited by M. Bate and A. Martinez Arias. Cold Spring Harbor Laboratory Press, Cold Spring Harbor, NY.

Wootton, J. C., R. E. Nicolson, J. M. Cock, D. E. Walters, J. F. Burke *et al.*, 1991 Enzymes depending on the pterin molybdenum cofactor: sequence families, spectroscopic properties of molybdenum and possible cofactor-binding domains. Biochim. Biophys. Acta **1057:** 157–185.

Yu, S.-Y., S. J. Yoo, L. Yang, C. Zapata, A. Srinivasan *et al.*, 2002 A pathway of signals regulating effector and initiator caspases in the developing *Drosophila* eye. Development **129:** 3269–3278.

Communicating editor: R. S. Hawley